Runge-Kutta discontinuous Galerkin finite element method for one-dimensional multimedium compressible flow

Rongsan Chen [+]

Department of Mathematics, Shanghai University, Shanghai 200444, P. R. China

Abstract. Runge-Kutta discontinuous Galerkin (RKDG) finite element method for hyperbolic conservation laws is a high order method, which can handle complicated geometries flexibly and treat boundary conditions easily. In this paper, we propose a new numerical method for treating interface using the advantages of RKDG finite element method. We use level set method to track the moving interface. In every time step, a Riemann problem at the interface is defined. The two cells adjacent to the interface are computed using the Riemann problem solver. If the interface crosses a cell in the next time step, the values of the flow variables of the cell crossed are modified through linear interpolation. Othewise, we do nothing.

Keywords: finite element, numerical analysis, Euler equation.

1. Introduction

The original discontinuous Galerkin (DG) finite element method was introduced by Reed and Hill [15] for solving the neutron transport equation. Runge-Kutta discontinuous Galerkin (RKDG) finite element method for no-linear hyperbolic conservation laws was proposed by Cockburn et al. [6, 5, 4, 7]. This method was constructed by using an explicit high order Runge-Kutta time discretization and piecewise linear DG method for space discretization. It can be designed for any order of accuracy in space and time, handle flexibly complicated geometries, and treat easily boundary conditions. Above all, the computation of any element depends only on the information of itself and its immediate neighbors, so it can be used easily for the efficient parrel implementation. RKDG finite element method performed very well for computation of the single-medium compressible flow. Various numerical schemes such as the total variation diminishing (TVD) schemes, the essentially non-oscillatory (ENO) or the weighted essentially non-oscillatory (WENO) schemes have been developed to solve single-medium flow, which can usually achieve high order accuracy with sharp and essentially non-oscillatory shock transition. However, when those schemes is directly applied to multi-medium flow, nonphysical oscillations usually occur in the vicinity of the material interface. In order to prevent oscillations near the interface, many methods were presented to treat the interface. The original ghost fluid method proposed by Fedkiw et al [8]. offers a fairly simple and flexible way to treat multi-medium interface and is easily extended to multi-dimension. In the GFM, one flow-field with two medium is separated into two flow-field by level set method, each of which has a single medium and can be computed solely. It was found to be less efficient when applied to gas-water flow or a strong shock wave interacting with the interface. This has resulted in many modified GFM [12, 11, 9, 17].

A Riemann problem based method for the resolution of compressible multi-material flow was proposed by Cocchi et al. [3]. The numerical algorithm consist of a predictor step and a correction step. In every time step, correction of the diffused nodes is carried out on both sides of the interface.

Several authors extended RKDG finite element method to multi-medium compressible flow. RKDG finite element for two-medium flow simulations in one and two dimension with the original GFM and the modified GFM were investigated by Qiu et al. [13]. Another important work of Qiu [14] is to use the RKDG finite element method for two-medium flow computation with conservative treatment of the moving material interface. R.S.Chen et al. computed multi-medium compressible flow by RKDG finite element with a new modified GFM [1, 2].

In this paper, we use RKDG finite element method for one dimension multi-medium compressible flow

---

[+] *Email address*: rschen@yahoo.cn

and use level set method to keep track of the interface location. In every time step, a Riemann problem at the interface is defined. The two cells adjacent to the interface is computed using the solver of the Riemann problem similar to the GFM, the other cells are computed by single-medium method. If the interface crosses a cell center at the next time step, the values of the cell crossed are modified by interpolation. Otherwise, we do nothing.

The paper is divided as follows. In section 2, Euler equations, equation of state (EOS),and level set equation are provided. In section 3, we first review the RKDG finite element method, and then we describe in detail the method of interface treatment. Tests on gas-gas and gas-liquid flow are given in section 4. In section 5, a brief conclusion is presented.

2. Equations

2.1. Euler Equations

The Euler equations for one-dimensional compressible flow are written as

$$\frac{\partial U}{\partial t} + \frac{\partial F(U)}{\partial x} = 0 \tag{2.1}$$

with $U = (\rho, \rho u, E)$, $F(U) = (\rho u, \rho u^2 + p, (E + p)u)$. Here ρ is the density, u is the velocity, p is the pressure, and E is the total energy for unit volume. The total energy is given as

$$E = \rho e + \frac{1}{2}\rho u^2 .$$

2.2. Equation of State (EOS)

For closure of the system, the EOS is required. We will use the following equation of state in this work.. The stiffened gas equation of state is in the form

$$p = (\gamma - 1)\rho e - \gamma p_\infty . \tag{2.2}$$

For γ-law gas, $p_\infty = 0$.

2.3. Level Set Equation

The level set method used o track the interface can be written as

$$\Phi_t(x,t) + u(x,t)\Phi_x(x,t) = 0 \tag{2.3}$$

Here u is the velocity of fluid. In general, $\Phi(x,t)$ starts out as a distance function. But over several time steps, it will not be equal to the distance function. In order to keep it as the signed distance function, the re-initialization step is necessary. In this work, the Riemann solver at the interface provides the accurate velocity of the interface, so we replace the $u(x,t)$ by interface velocity and the re-initialization is not implemented. The level set equation is solved by the integral-averaging scheme proposed by Liu et al. [10].

3. RKDG finite element method

3.1 Description RKDG finite element method

The computational domain R is divided into N cells, $R = \cup_i I_i$, where $I_i = (x_{i-1/2}, x_{i+1/2})$, $i = 1,2,\cdots,N$. Denote the cell centers by $x_i = \dfrac{x_{i-1/2} + x_{i+1/2}}{2}$ and the cell sizes by $\Delta x_i = (x_{i+1/2} - x_{i-1/2})$. Let us define

$$U_h = V_h = V_h^k = \left\{ p \in BV \bigcap L^1 : p\big|_{I_i} \in P^k(I_i) \right\}$$

Where U_h is solution space, V_h is test function space, and $P^k(I_i)$ is the space of polynomials of degree $\leq k$ on I_i. We use a local orthogonal basis over I_i, $\{v_l^i(x), l = 0,1,\cdots,k\}$. We choose for example

$$v_0^i(x) = 1, v_1^i(x) = \frac{x - x_i}{\Delta x_i / 2}, v_2^i(x) = \frac{1}{2}\left(3\left(\frac{x - x_i}{\Delta x_i / 2}\right)^2 - 1\right), \cdots \tag{3.1}$$

The approximate solution U_h can be written as

$$U_h(x,t) = \sum_{l=0}^{k} U_i^l(t) v_l^i(x) \quad \text{for } x \in I_i. \tag{3.2}$$

Where $\left\{U_i^l\right\}_{l=0}^{k}$ are the degrees of freedom.

We substitute (3.2) into (2.1), multiply by $v_l^i(x)$, integrate over a cell I_i and integrate by parts:

$$\frac{d}{dt}U_i^l(t) - \frac{1}{\Delta x_i / (2l+1)}\left(-\int_{I_i} F(U_h(x,t))\frac{d}{dx}v_l^i(x)dx \right.$$
$$\left. + F(U_h(x_{i+1/2},t)) - F(U_h(x_{i-1/2},t))\right) = 0, \tag{3.3}$$
$$l = 0,1,\cdots,k.$$

The flux $F(U_h(x_{i+1/2},t))$ is usually replaced by a monotone numerical flux $H(U_{i+1/2}^-, U_{i+1/2}^+)$, where $U_{i+1/2}^{\pm} = U_h(x_{i+1/2}^{\pm},t)$, resulting in the scheme:

$$\frac{d}{dt}U_i^l(t) - \frac{1}{\Delta x_i / (2l+1)}\left(-\int_{I_i} F(U_h(x,t))\frac{d}{dx}v_l^i(x)dx \right.$$
$$\left. + H(U_{i+1/2}^-, U_{i+1/2}^+) - H(U_{i-1/2}^-, U_{i-1/2}^+)\right) = 0, \tag{3.4}$$
$$l = 0,1,\cdots,k.$$

We use the local Lax-Friedrichs flux

$$H(U_{i+1/2}^-, U_{i+1/2}^+) = \frac{1}{2}\left[F(U_{i+1/2}^-) + F(U_{i+1/2}^+) - \alpha_{i+1/2}(U_{i+1/2}^+ - U_{i+1/2}^-)\right],$$

with

$$\alpha_{i+1/2} = \max_{1 \le p \le 3}\left(\left|\lambda_{i+1/2}^{(p)+}\right|, \left|\lambda_{i+1/2}^{(p)-}\right|\right),$$

where $|\lambda_{i+1/2}^{(p)\pm}|$, $p = 1, 2, 3$, are the 3 real eigenvalues of the Jacobian $(\frac{\partial F}{\partial U})_{U = U_{i+1/2}^{\pm}}$.

At last, the semi-discrete scheme can be written as

$$\frac{d}{dt}U_h = L_h(U_h). \tag{3.5}$$

We discrete (3.5) by Runge-Kutta method. In order to achieve variation stability, a slope limiter is used after each Runge-Kutta stage. For a complete discussion of the method, the reader is referred to [6].

3.2 Treatment of interface

The cell sizes are uniform, we denote the cell centers by x_i, denote Φ_i^n by the level set function value of x_i at $t = t_n$, denote x_I^n by the interface location at $t = t_n$. Assuming the interface x_I^n is between x_i and x_{i+1}, the left of interface is fluid 1, and the right of interface is fluid 2. At instance $t = t_{n+1}$, three instance may occur: (1) x_I^{n+1} is between x_i and x_{i+1}, as shown Fig.1 (a); (2) x_I^{n+1} is between x_{i-1} and x_i, as shown Fig.1 (b); (3) x_I^{n+1} is between x_{i+1} and x_{i+2}, as shown Fig.1 (c). Supposed that the flow states at $t = t_n$ have been known, the following steps are taken to obtain the respective quantities at the next step:
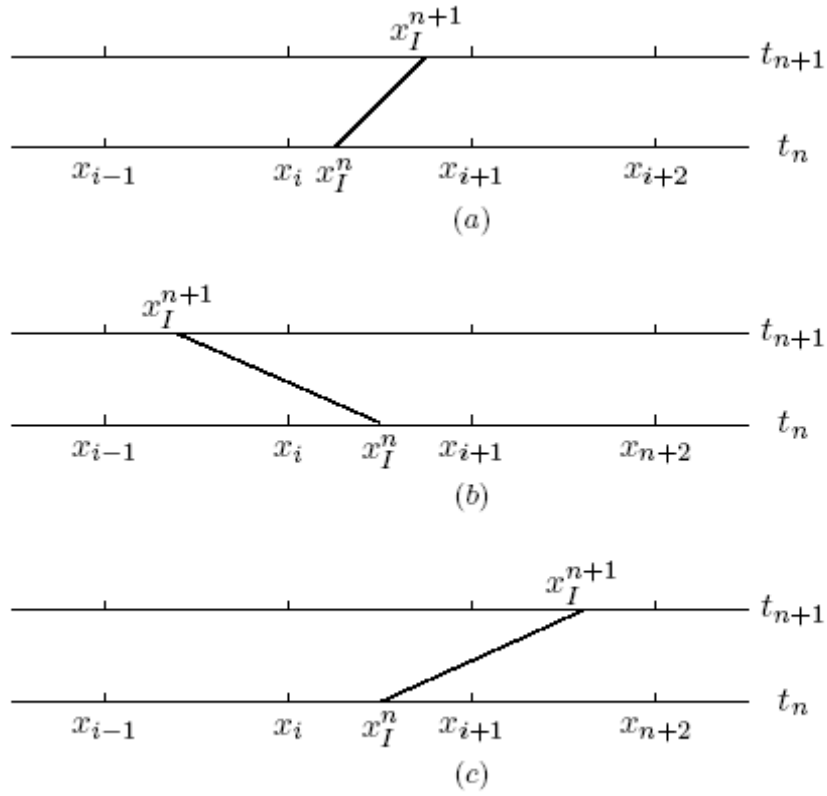
Fig.1

1. Define Riemann problem

$$\begin{cases} \dfrac{\partial U}{\partial t} + \dfrac{\partial F(U)}{\partial x} = 0 \\ U(x,t_n) = \begin{cases} U_{i-1}^n, x < x_I^n \\ U_{i+2}^n, x > x_I^n \end{cases} \end{cases} \tag{3.6}$$

Solve the Riemann problem, we can get u_I (the velocity of interface), p_I (the pressure of interface), ρ_{IL} (the density of the left of interface), ρ_{IR} (the density of the right of interface), S_{IL} (the entropy of the left of interface), S_{IR} (the entropy of the right of interface). We denote

$$U_{IL} = (\rho_{IL}, \rho_{IL}u_I, E_{IL}), U_{IR} = (\rho_{IR}, \rho_{IR}u_I, E_{IR}) \ .$$

2. The isobaric fix technique can be used to reduced the "overheating" errors [7]. This is done by

$$S_i = S_{IL}, S_{i+1} = S_{IR}$$

3. For the cells $I_1, I_2, \cdots, I_i$, use EOS of Fluid 1; For the cells $I_{i+1}, I_{i+2}, \cdots, I_N$, use EOS of Fluid 2. We can compute the flow at $I_1, I_2, \cdots, I_{i-1}, I_{i+2}, \cdots, I_N$ as for single-medium flow. But the cells I_i and I_{i+1} must be treated specially. When we compute flow at cell I_i , we can't use the flow state at I_{i+1} directly because they belong to different fluids. So we modify it as below: if we compute at I_i , $H(U_{i+1/2}^-, U_{i+1/2}^+) = H(U_{i+1/2}^-, U_{IL})$. If we compute at I_{i+1} , similar as at I_i, $H(U_{i+1/2}^-, U_{i+1/2}^+) = H(U_{IR}, U_{i+1/2}^+)$

4. Solve the level set equation using u_I , we can obtain $\Phi(x, t_{n+1})$.

5. If $x_I^{n+1} \in [x_i, x_{i+1}]$, we do nothing. If $x_I^{n+1} \in [x_{i-1}, x_i]$, we obtain U_i^{n+1} by interpolation: for constant interpolation

$$U_i^{n+1} = U_{IR}, \tag{3.7}$$

or for linear interpolation,

$$U_i^{n+1} = \frac{U_{i+1}^{n+1} - U_{IR}}{\Phi_{i+1}^{n+1}} \Phi_i^{n+1} + U_{IR}. \tag{3.8}$$

If $x_I^{n+1} \in [x_{i+1}, x_{i+2}]$, we obtain U_i^{n+1} by interpolation:

for constant interpolation,

$$U_i^{n+1} = U_{IL}, \tag{3.9}$$

or for linear interpolation,

$$U_i^{n+1} = \frac{U_{i-1}^{n+1} - U_{IL}}{\Phi_{i-1}^{n+1}} \Phi_i^{n+1} + U_{IL}. \tag{3.10}$$
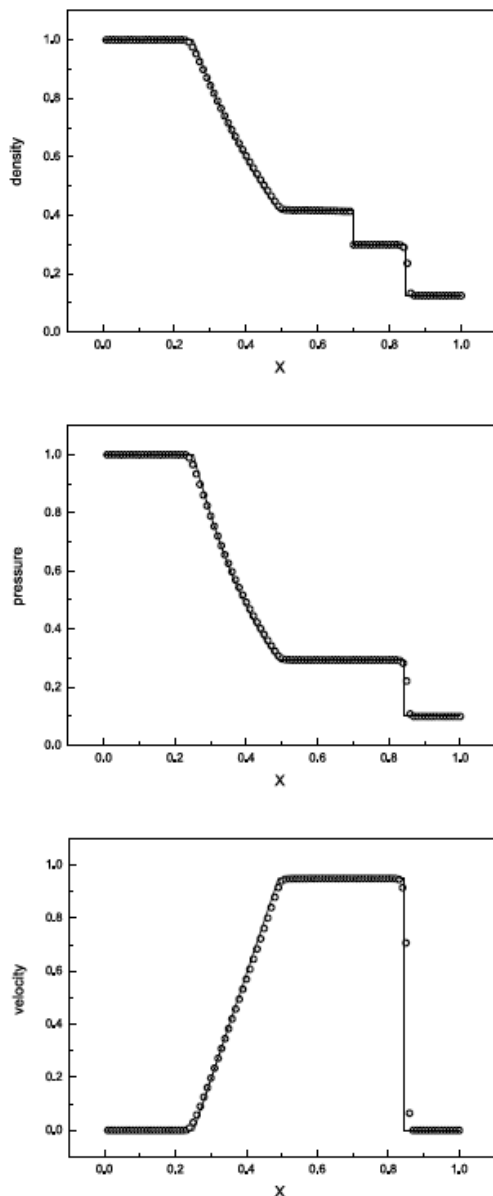
The solution can be advanced from U^n to U^{n+1}.

4. Numerical results

Fig.2 Example 1, 100 cells
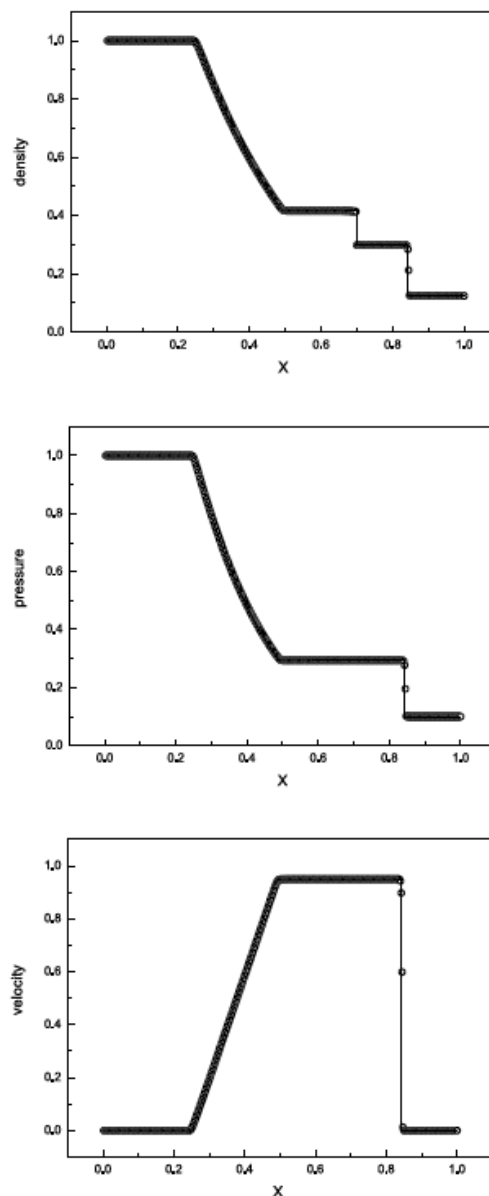
Fig.3 Example 1, 400 cells

In this section, five numerical experiments are presented. For the computations, CFL is set to 0.2, computational domain is [0, 1], the solid line is the exact solution and the points are the computed solution. A third order accurate RKDG finite element method is used to solve the Euler equation.

Example 4.1 This is a gaseous shock tube problem taken from [17] and the initial conditions are

$$(\rho, u, p, \gamma) = \begin{cases} (1,0,1,1.4,0), & if \quad 0 \le x < 0.5, \\ (0.125,0,0.1,1.2,0), & if \quad 0.5 < x \le 1. \end{cases}$$

The computational time is $t = 0.21$. Fig.2 shows the result of 100 mesh points, and Fig.3 shows the result of 400 mesh points. From the Figs. 2-3, we see that there are no-physical oscillation near the interface and the computed solutions concur with the exact solutions.

Example 4.2 We consider a two-phase gas-liquid Riemann problem which is taken from [16]. The initial states are defined as

$$(\rho, u, p, \gamma) = \begin{cases} (1.241,0,2.753,1.4,0), & if \quad 0 \le x < 0.5, \\ (0.991,0,3.059 \times 10^{-4},5.5,1.505), & if \quad 0.5 < x \le 1. \end{cases}$$
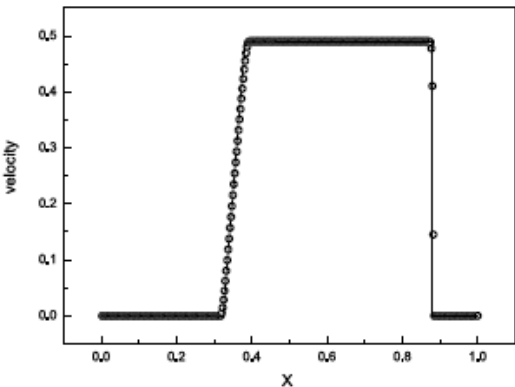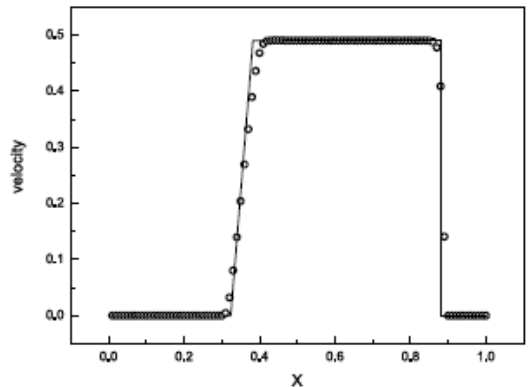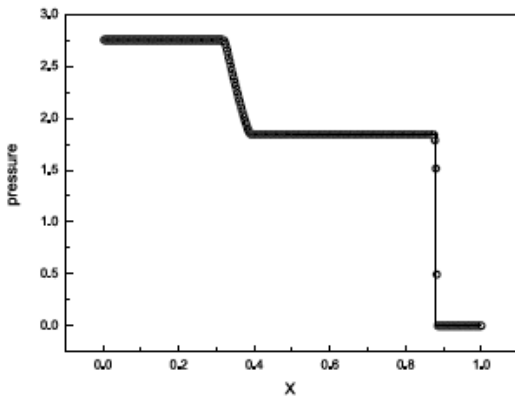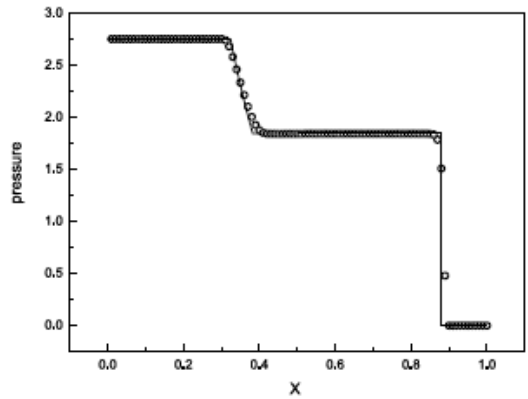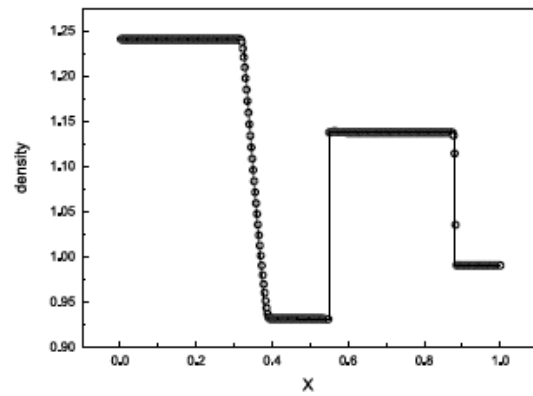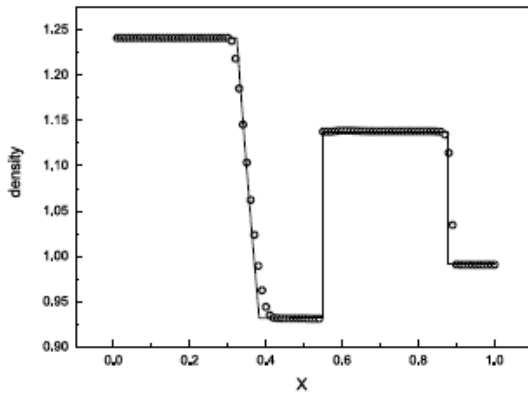
Fig.4 Example 2, 100 cells   Fig.5 Example 2, 400 cells

The results of 100 mesh points and 400 mesh points at $t = 0.1$ are shown in Figs.4-5. The computational solutions are convergent to physical solutions as the mesh refined.

Example 4.3 A gas-liquid shock tube problem is taken from [9]. The initial conditions are

$$(\rho, u, p, \gamma) = \begin{cases} (0.5, 100, 20000, 2.5, 0), & if \quad 0 \leq x < 0.5, \\ (1, 0, 1, 7.15, 3309), & if \quad 0.5 < x \leq 1. \end{cases}$$

Shown in Figs.6-7 are the respective results obtained by 100 mesh points and 400 mesh points at time $t = 0.001$ that agree with the exact solutions.
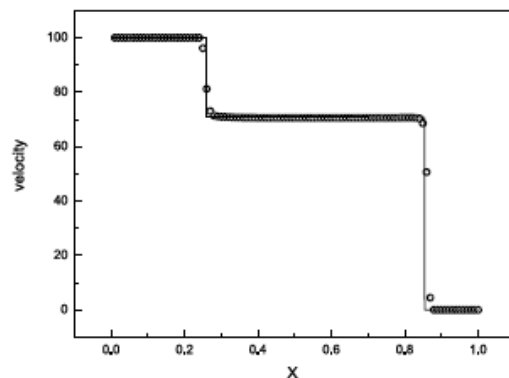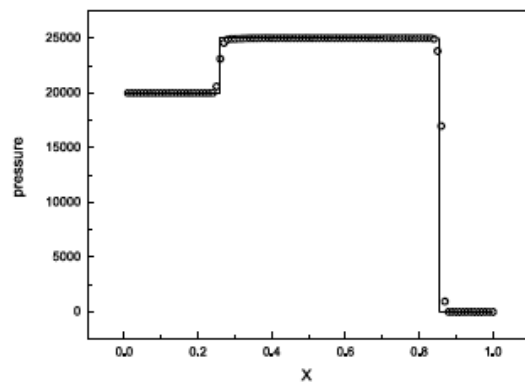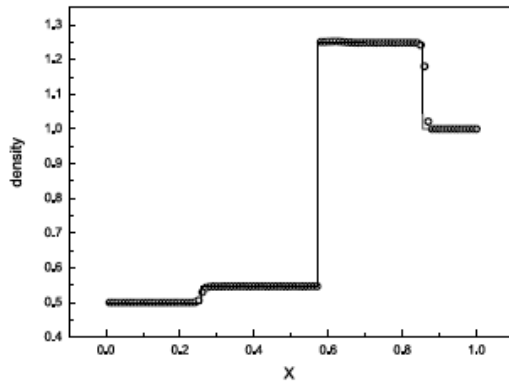
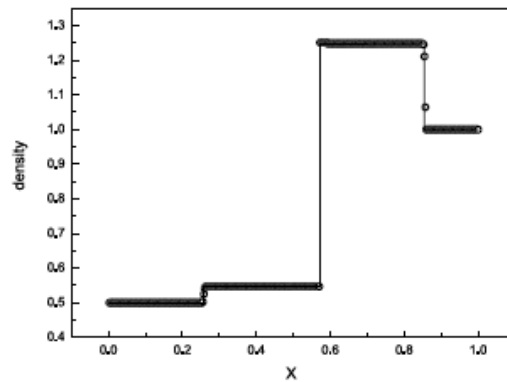Fig.6 Example 3, 100 cells   Fig.7 Example 3, 400 cells
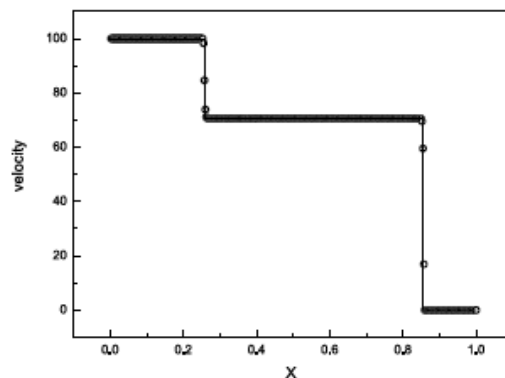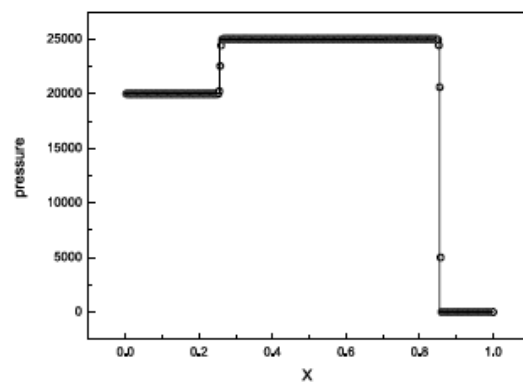
Example 4.4 We consider strong shock impacting on a gas-water interface which is taken from [17]. The initial position of shock and interface are the same at . The initial condition are as follows:

$$(\rho, u, p, \gamma) = \begin{cases} (0.00596521, 911.8821, 1000, 1.4, 0), & if \quad 0 \leq x < 0.5, \\ (1, 0, 1, 7.15, 3309), & if \quad 0.5 < x \leq 1. \end{cases}$$

The results at $t = 0.0007$ are presented in Figs.6-7. The position of shock and interface are predicted accurately.

Example 4.5 Jet impact on the gas-water interface is considered. This is taken from [17]. The initial condition are given as

$$(\rho, u, p, \gamma) = \begin{cases} (1, 90, 1, 1.4, 0), & if \quad 0 \le x < 0.5, \\ (1000, 0, 1, 7.15, 3309), & if \quad 0.5 < x \le 1. \end{cases}$$

This is a very difficult problem. The results of 100 mesh points and 400 mesh points at $t = 0.015$ are obtained, shown in Figs.7-8. The results show that the shock wave and the interface are well located.
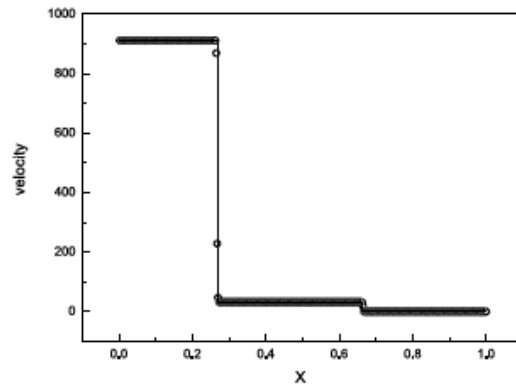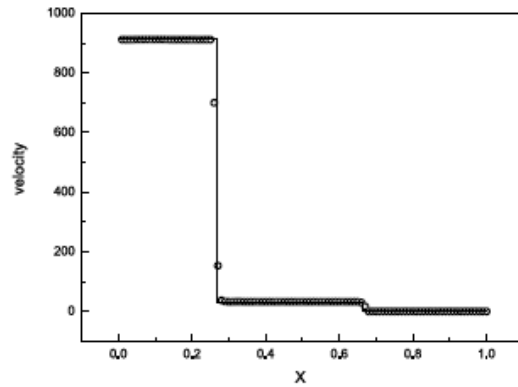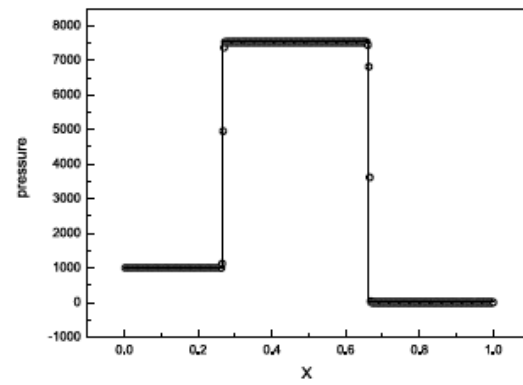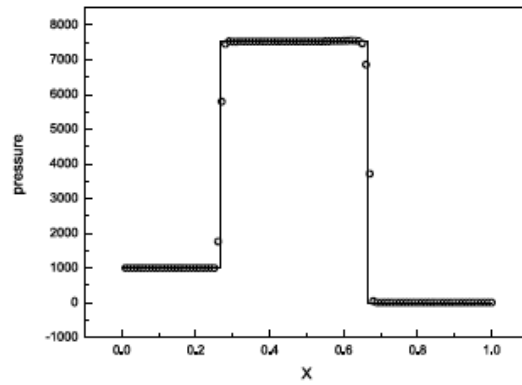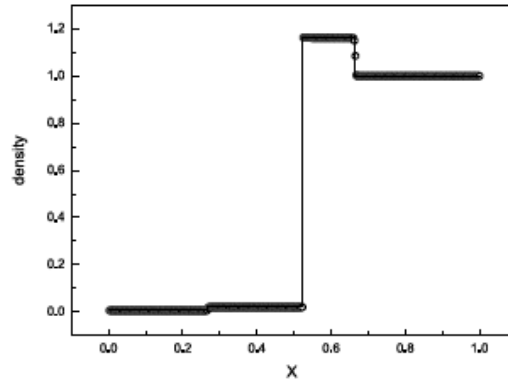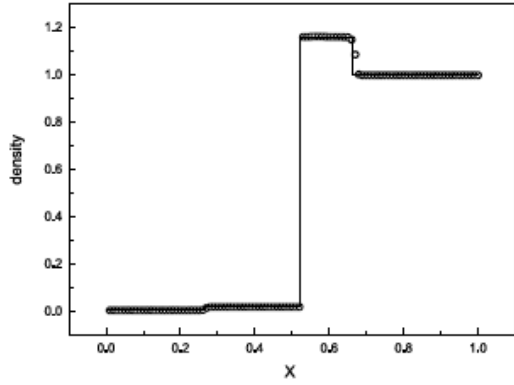

Fig.8 Example 4, 100 cells   Fig.9 Example 4, 400 cells
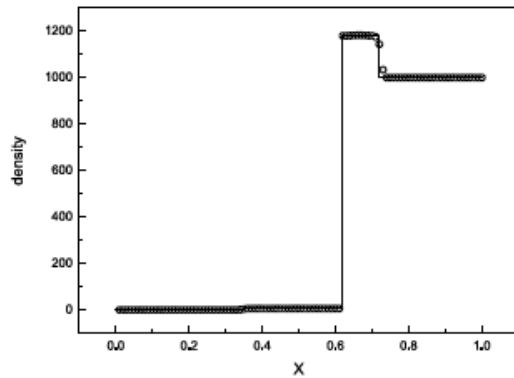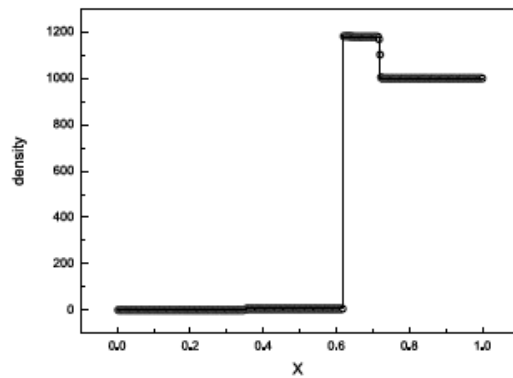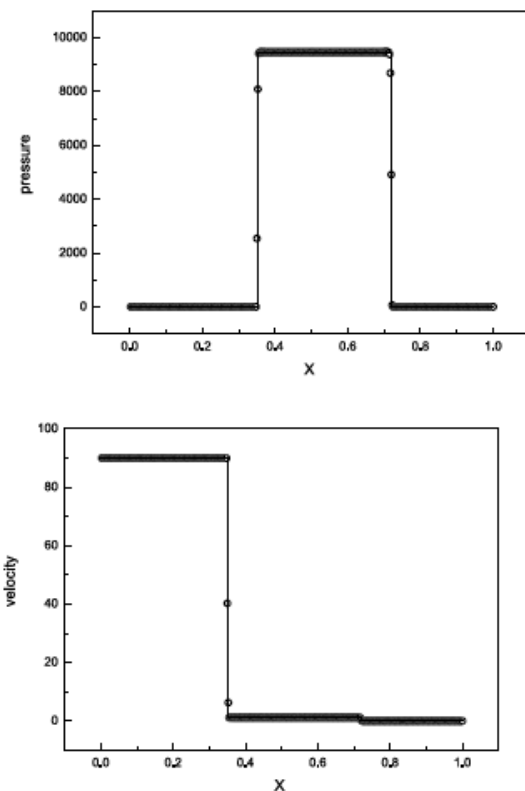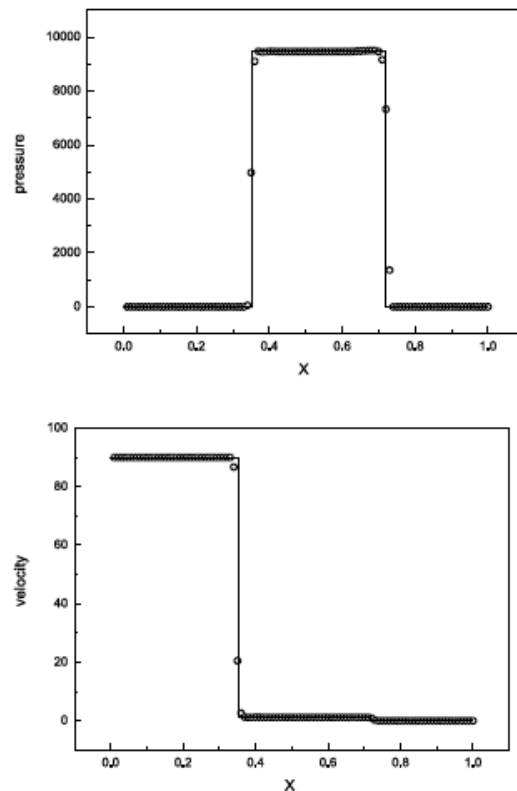
Fig.10 Example 5, 100 cells   Fig.11 Example 5, 400 cells

5. Conclusions

In this paper, RKDG finite element methods with a new treatment of the moving interface have been developed to simulate one-dimensional multi-medium compressible flow. At every time step, a Riemann problem at the interface is defined, the two cells near interface are computed using the solver of Riemann problem. If the interface crosses a cell, we modify the values of the cell crossed by interpolation. This method is very simple. Compared with GFM method, it cost less. Numerical results for gas-gas and gas-liquid flow in one dimension show the present method is robust. Ongoing work is to extend these methods for two dimension.

6. References

[1]   R. S. Chen, X. J. Yu, A high order accurate RKDG finite element method for one dimensional compressible multicomponent Euler equation. *Chinese J. Comput. Phys*. 2006, **23**: 43–49.

[2]   R. S. Chen, X. J. Yu, An RKDG finite element method for two dimensional compressible multimedia fluids. *Chinese J. Comput. Phys*. 2006, **23** : 699–705.

[3]   J.-P. Cocchi, R. Saurel, A Riemann problem based method for the resolution of compressible multimaterial flows. *J. Comput. Phys*. 1997, **137**: 265–298.

[4]   B. Cockburn, S. Hou, C.-W. Shu, TVB Runge-Kutta local projecting discontinuous Galerkin finite element methods for conservation laws IV: the multidimensional case. *J. Comput. Math. Comp*. 1990, **54**: 541–581.

[5]   B. Cockburn, S.-Y. Lin, C.-W. Shu, TVB Runge-Kutta local projecting discontinuous Galerkin finite element methods for conservation laws III: one dimensional systems. *J. Comput. Phys*. 1989, **84**: 90–113.

[6]   B. Cockburn, C.-W. Shu, TVB Runge-Kutta local projecting discontinuous Galerkin finite element methods for conservation laws II: general framework. *Math. Comp*. 1989, **52**: 411–435.

[7]   B. Cockburn, C.-W. Shu, TVB Runge-Kutta local projecting discontinuous Galerkin finite element methods for conservation laws V: multidimensional systems. *J. Comput. Phys*. 1998, **141**: 199–224.

[8]   R. P. Fedkiw, B. T. Aslam, S.osher, A non-oscillatory Eulerian approach to interfaces in multimaterial flows (the ghost fluid method), *J. Comput. Phys*. 1999, **152**: 457–492.

[9]   X. Y. Hu, B. C. Khoo, An interface interaction method for compressible multifluids. *J. Comput. Phys*. 2004, **198**: 35–64.

[10] R. X. Liu, X. P. Liu, L. Zhang, Z. F. Wang, Tracking and rescontruction methods for moving-interface. *Appl. Math. Mech*. 2004, **25**: 307–321.

[11] T. G. Liu, B. C. Khoo, C. Wang, The ghost fluid method for compressible gas-water simulation. *J. Comput. Phys*. 2005, **204**: 193–221.

[12] T. G. Liu, B. C. Khoo, K. S. Yeo, Ghost fluid method for strong shock impacting on material interface. *J. Comput. Phys*. 2003, **190**: 651–681.

[13] J. X. Qiu, T. Liu, B.C.khoo, Simulations of compressible two-medium flow by Runge-Kutta discontinuous Galerkin methods with the ghost fluid method. *Commun. Comput. Phys*. 2008, **3**: 479–504.

[14] J. X. Qiu, T. G. Liu, B. C. Khoo, Runge-Kutta Discontinuous Galerkin methods for compressible two-medium flow simulations: one-dimensional case. *J. Comput. Phys*. 2007, **222**: 353–373.

[15] W. H. Reed, T. R. Hill, Triangular mesh methods for the neutron transport equation. *Tech. rep*. Los Alamos Scienfic Laboratory Report LA-UR-(1973).

[16] K. M. Shyue, An efficient shock-capturing algorithm for compressible multicomponent problems. *J. Comput. Phys*. 1998, **142**: 208–242.

[17] C. W. Wang, T. G. Liu, B. C. Khoo, A real-ghost fluid method for the simulation of multi-medium compressible flow. *SIAM J. Sci. Comput*. 2006, **28**: 278–302.